International Review of Economics and Finance 97 (2025) 103830

Contents lists available at ScienceDirect

International Review of Economics and Finance

journal homepage: www.elsevier.com/locate/iref

Information loss from perception alignment

Omid M. Ardakani [a,*], Viktoria Dalko [b,c], Hyeeun Shim [d]

[a] Parker College of Business, Georgia Southern University, United States of America
[b] Hult International Business School, United States of America
[c] Harvard University, United States of America
[d] AffyXell Therapeutics, Republic of Korea

ARTICLE INFO

JEL classification:
G14
G17
G12

Keywords:
Information theory
Perception alignment
Divergence measures

ABSTRACT

This paper examines how synchronized investor perceptions of future asset returns affect market information dynamics. We introduce an empirical framework that applies information-theoretic measures, such as Kullback–Leibler and Jensen–Shannon divergences, to quantify the extent of perception alignment among investors and its impact on information loss. The findings show that heightened perception alignment increases information loss, especially during the COVID-19 pandemic. The findings emphasize our ability to measure information loss and capture shifts in investor behavior, with applications extending to various markets and events.

Introduction

Investor decisions in financial markets are profoundly influenced by their perceptions of future market trends and potential returns, often leading to synchronized behaviors. Such alignment can be precipitated by various factors, including public news dissemination and cognitive biases. The effect of perception alignment on market dynamics can destabilize market equilibrium and affect price stability. Recent literature in behavioral finance has shown that understanding these synchronized behaviors provides deeper insights into the collective decision-making processes that drive financial markets (Devenow & Welch, 1996; Hirshleifer, 2001). These studies challenge traditional views by demonstrating how information and belief convergence among traders can lead to significant market movements and volatility. This paper studies perception alignment by employing information-theoretic approaches to quantify these phenomena and evaluate their implications on market stability and investor behavior during periods of high uncertainty. Specifically, spurious herding which is induced by perception alignment highlights how synchronized reactions to public news can lead to collective market movements without deliberate imitation among investors.

Recent studies examine how investor perceptions align and the ensuing effects on market behavior (Clements et al., 2017; Hirshleifer et al., 2009; Hwang & Salmon, 2001; Khwaja & Mian, 2005; Klein et al., 2012; Wermers, 1999). The perception alignment hypothesis posits that news, when credible and widely disseminated, can synchronize investor perceptions. This hypothesis is central to understanding the mechanics through which information dissemination impacts investor decision-making and market outcomes. Empirical and theoretical advancements have examined the extent to which shared beliefs among investors lead to collective movements in market prices, further revealing connections between information, perception, and market behavior (Dasgupta et al., 2011; Foucault et al., 2017; Hirshleifer et al., 2021).

* Corresponding author.
E-mail addresses: oardakani@georgiasouthern.edu (O.M. Ardakani), viktoria.dalko@faculty.hult.edu (V. Dalko), hs09786@georgiasouthern.edu (H. Shim).

https://doi.org/10.1016/j.iref.2024.103830
Received 18 September 2023; Received in revised form 27 October 2024; Accepted 17 December 2024
Available online 24 December 2024

The recent literature encompasses econometric approaches that have been employed to capture and quantify perception alignment in high-frequency trading environments. Methods such as the use of ensemble learning methods to improve forecast accuracy (Cohen, 2022) and deep learning models to analyze investor sentiment from large-scale data (Mansurov et al., 2023) are a few examples. The integration of recurrent neural networks to model temporal dynamics in market data also offers insights into how collective investor behaviors evolve (Chacon et al., 2020; Hashemi et al., 2022). These approaches reflect the latest efforts in empirical research and tie into our methodological framework, which leverages information-theoretic measures to assess perception alignment. Chang et al. (2000) and Galarioitis et al. (2015) also provide perspectives on the impact of fundamental information and illustrate the various contexts in which investors expectations can affect market dynamics. Research on closed-end fund investors (Cui et al., 2019) and studies on disagreement influences asset prices (Carlin et al., 2014) further improve our understanding of market behavior under different informational influences.

This paper studies perception alignment by introducing a methodological framework that leverages divergence measures. We employ the Kullback–Leibler divergence (KLD) and other related measures, such as Jensen–Shannon and Rényi divergences, to evaluate the degree to which individual investor forecasts align with collective market sentiment or an idealized theoretical model. This is accomplished by first calculating out-of-sample forecast errors using an optimal autoregressive integrated moving average model on a rolling forecasting basis. We then apply these divergence measures to compare the empirical probability distributions of forecast errors against those derived from a hypothetical perfect forecast model. Specifically, divergence measures, including KLD provides a measure of the information loss when transitioning from an actual distribution of forecast errors to an ideal one. It quantifies how closely investors' perceptions align under varying market conditions influenced by external news. A decrease in KLD, supplemented by Jensen–Shannon divergence, indicates a higher degree of alignment.

This research contributes to the understanding of perception alignment under information asymmetry. By integrating Cross-Sectional Absolute Deviation (CSAD) with KLD, we can extend the framework to analyze perception alignment. This approach is informed by insights from Chang et al. (2000) and Galarioitis et al. (2015), which highlight the importance of macroeconomic information and the differentiation between spurious and intentional herding. Our empirical study examines the dynamics of financial markets during the COVID-19 pandemic. We first leverage the minute-by-minute CBOE Volatility Index (VIX) from January 22, 2020, to April 24, 2020, to study the alignment of investor perceptions under extreme events. During this period, we observed significant fluctuations in the VIX, particularly following the World Health Organization's declaration of the pandemic. We also include the Australian Securities Exchange S&P/ASX 200 index during the sharp market sell-off in March 2020. The findings indicate a tendency towards alignment of investors expectations, especially in times of high uncertainty. This behavior is characterized by investors moving collectively in response to new information, which leads to a more aligned perception of market risks and future returns. This alignment can be seen in the reduction of the KLD post-pandemic announcement, suggesting a closer fit between observed data and theoretical models of market behavior.

The organization of this paper is as follows. Section 1 reviews the literature on perception alignment and different types of herding. Section 2 first discusses the divergence measures and their properties and develops a framework to capture investors' perceptions about future prices. Through examples and simulation studies, this section shows how perception alignment leads to an increase in information loss and incorporates cross-sectional absolute deviation of returns with divergence measures. Section 3 presents empirical evidence on perception alignment using high-frequency VIX returns during the pandemic and explores a recent incident of perception alignment on Australia's securities exchange. Section 4 discusses the empirical findings and compares them in the context of existing literature. Finally, Section 5 provides some concluding remarks.

1. Background

Investor behavior reflects a mixture of individual decision-making and responses to collective market dynamics. Among factors influencing these behaviors, perception alignment is distinguished as driving market movements and investor interactions. This convergence of expectations and beliefs among market participants, often catalyzed by shared information or significant economic events, can lead to pronounced herding behavior. This section reviews how perception alignment facilitates understanding market trends and underscores the susceptibility of markets to misinformation.

1.1. Perception alignment

Perception alignment refers to the phenomenon where investors' expectations and beliefs about future market behaviors converge towards a common outlook influenced by shared information or prevailing market sentiments. This convergence is associated with herding potentially sidelining their independent judgment or private information (Banerjee, 1992; Bikhchandani et al., 1992). Perception alignment determines how collective behaviors can drive significant market movements. Empirical studies have demonstrated that perception alignment can be triggered by both macroeconomic announcements and firm-specific information. For example, Andersen et al. (2003) and Andersen et al. (2007) show that foreign exchange markets react to macroeconomic news. Their findings suggest that investors align their perceptions based on new information. Similarly, Chang et al. (2000) found pronounced herding behavior in the Korean and Taiwanese equity markets, heavily influenced by macroeconomic rather than firm-specific news, indicating a strong component of perception alignment driven by broader economic indicators.

Perception alignment can also lead to artificial price movements and potentially severe financial crises. Notable historical instances include massive market crashes following orchestrated panic selling of the Brazilian stock markets in 1989 and the Bombay Stock Exchange in 2001 (Carvajal & Elliott, 2009; GFD, 2009). The flash crashes on the New York Stock Exchange in 2010 and the

National Stock Exchange of India in 2012 are prime examples of how large orders and technical errors can trigger widespread herding, leading to significant market drops within minutes (Dalko & Wang, 2019). These events highlight the susceptibility of financial markets to rapid perception alignment in response to sudden market shocks (Dalko & Wang, 2020).

Recent research has explored the ways in which global events and market disruptions influence perception alignment across different financial contexts. For example, Kizys et al. (2021) and Tan et al. (2021) document perception alignment in international stock markets triggered during the COVID-19 pandemic. Such events highlight the impacts of external shocks on market movements through the alignment of investor perceptions. The literature has documented models that indicate how social dynamics and the flow of information can lead to this convergence in investors' expectations (Avery & Zemsky, 1998; Welch, 1992). These models underscore the influence of public and private information in shaping the market consensus that guides investor behavior. Quantitative measures of perception alignment have been developed to assess how closely the beliefs of different investors mirror each other or a common trend (Hwang & Salmon, 2001). More recently, advanced econometric models have been employed to quantify the degree of alignment, examining how investor sentiments synchronize in response to news or market events (Allen & Gale, 1992; Babii et al., 2022; Casoli & Lucchetti, 2022; Rossi et al., 2015).

1.2. Herding

Herding refers to investors' behavior when following others' trades or investment strategies rather than relying on their independent information. Herding represents a manifestation of how aligned perceptions among investors can translate into collective action. While both perception alignment and herding concern investor behaviors, they describe distinct aspects of these behaviors. Perception alignment refers to the convergence of expectations among investors. This convergence is often driven by shared information or reactions to market events. In contrast, herding is defined as the collective action taken by investors, where individual decision-making is often overshadowed by the inclination to follow the majority. This is documented across diverse market environments globally, reflecting both rational and irrational motives behind investor decisions. For example, herding literature studies the U.S. (Barber et al., 2006; Christie & Huang, 1995), the U.K. (Hwang & Salmon, 2001), Japan (Hwang & Salmon, 2001), Germany (Dorn et al., 2008), France (Merli & Roger, 2013), Italy (Caparrelli et al., 2004), Israel (Venezia et al., 2011), South Korea (Choe et al., 1999), Taiwan (Chang et al., 2000), Indonesia (Bowe & Domuta, 2004), and China (Tan et al., 2008). The recent contributions to this literature focus on different types of herding.

Informational herding is a form of market behavior where investors follow the trades of others, assuming these individuals have access to superior information (Bohren, 2016; Smith et al., 2021). This is prevalent in environments characterized by high uncertainty and asymmetric information. The rationale behind informational herding stems from the natural human response to uncertainty; investors often perceive that following informed agents reduces the potential for significant losses associated with making unilateral decisions based on limited or noisy information. Foucault et al. (2017) find that in conditions where asset values are highly uncertain, traders significantly increase their propensity to mimic the actions of others, leading to increased market volatility and price distortions. Vayanos and Woolley (2013) study the dynamic interactions between informational herding and market liquidity, showing herding can lead to liquidity spirals where initial herding actions cause price overreactions, which in turn attract additional herding, thus exacerbating initial mispricings. Dasgupta et al. (2011) extend it to examine how investors engage in cross-market herding in response to global signals and local cues, finding that such behavior can lead to synchronized market movements and potential global financial instabilities.

Spurious herding is a dynamic in which the actions of investors are correlated not due to intentional imitation but because of their common reactions to external stimuli, such as public news or global events. This type of herding is primarily driven by perception alignment, where synchronized expectations and beliefs, shaped by shared information, inadvertently lead to uniform market movements. The influence of global news on market behavior can lead to such correlated behaviors across different markets (Di Giovanni & Hale, 2022). Although this collective adjustment of portfolios is a response to new information, it is not a deliberate decision to follow others. Kizys et al. (2021) illustrate the impact of macroeconomic news on stock prices and trading volumes, particularly during periods of significant news releases, even in the absence of direct investor communication. This suggests that spurious herding which is caused by perception alignment occurs as investors react similarly to new information. Filip and Pochea (2023) also suggest that the accelerating pace at which financial news is disseminated globally may enhance the synchronization of market reactions. This synchronization spreads information and intensifies market volatility, which highlights the consequences of spurious herding driven by perception alignment.

Behavioral herding is primarily influenced by psychological factors such as investor sentiment. Unlike informational or spurious herding, behavioral herding stems from the intrinsic human tendency to follow the crowd, often disregarding individual analytical judgments or factual information. This type of herding is particularly potent during periods of high market volatility and uncertainty, where emotional responses can dominate rational decision-making. Shiller (2000) highlights how collective emotional states can lead to excessive market rallies or crashes, illustrating behavioral herding through panic selling or irrational exuberance. Further empirical evidence illustrates that investors are more likely to engage in herding when faced with ambiguous information and heightened emotional states, leading to significant market movements based purely on sentiment rather than new economic data (Hirshleifer & Teoh, 2017). Baker and Wurgler (2007) expands on this by demonstrating that high levels of investor sentiment tend to precede low future returns, reinforcing the notion that behavioral herding can distort asset prices away from their fundamental values.

Reputational herding occurs when investment managers conform to the actions of their peers, driven by concerns over career risks rather than direct financial incentives (Roider & Voskort, 2016). This type of herding is dominant among fund managers

Table 1
Summary of herding types.

Type of herding	Cause of herding	Key references
Informational	Driven by asymmetric information, investors follow those presumed to have superior information.	Bohren (2016), Dasgupta et al. (2011), Foucault et al. (2017), Smith et al. (2021) and Vayanos and Woolley (2013)
Spurious	Caused by synchronized reactions to external stimuli rather than intentional imitation.	Di Giovanni and Hale (2022), Filip and Pochea (2023) and Kizys et al. (2021)
Behavioral	Influenced by psychological factors, especially under high market volatility and uncertainty.	Baker and Wurgler (2007), Hirshleifer and Teoh (2017) and Shiller (2000)
Reputational	Occurs among fund managers due to career concerns over job security and professional reputation.	Boyson (2010), Chevalier and Ellison (1999), Roider and Voskort (2016) and Sias (2004)
Strategic	Investors deliberately follow others to capitalize on perceived profitable opportunities or to mitigate risks.	Banerjee (1992), Bikhchandani et al. (1992), Blasco and Ferreruela (2008), Cipriani and Guarino (2014) and Gavriilidis et al. (2013)

who operate in highly competitive or volatile markets, where the cost of underperformance can extend beyond financial loss to include job security and professional reputation (Boyson, 2010). Sias (2004) highlights that the higher pressure to conform can reduce the variance of a manager's performance relative to the benchmark and peers. While this may mitigate the risk of relative underperformance, it comes at the cost of forsaking higher potential returns from alternative investment strategies. Chevalier and Ellison (1999) also find that younger managers, more concerned with establishing a reputation, are more likely to herd than their more established counterparts. This behavior is indicative of strategic career concerns that can distort investment decisions, leading to suboptimal portfolio performance. Moreover, Dasgupta et al. (2011) suggest that global fund managers often engage in herding not only within their domestic markets but also in foreign equities, particularly in regions where peer performance is highly visible and comparably scrutinized.

Strategic herding represents a deliberate form of market behavior where investors choose to follow the trades of others to capitalize on perceived profitable opportunities or to avoid potential losses. This type of herding is observed when investors believe that aligning their trades with market leaders or trendsetters can yield significant gains or mitigate risks during volatile periods (Blasco & Ferreruela, 2008; Gavriilidis et al., 2013). Cipriani and Guarino (2014) indicate that traders engage in herding not necessarily because they possess or observe superior information but because they anticipate that following the actions of others can lead to advantageous outcomes, especially when market trends are strong and clear. This behavior underscores the rational calculations involved in strategic herding, where the benefits of mimicking others' trades outweigh the potential risks of independent action. Banerjee (1992) suggests that when individuals observe others making certain choices, they infer that those choices are based on private information, prompting them to follow suit even without direct knowledge of such information. This inclination can lead to cascades where, once a mass is reached, subsequent traders blindly follow the herd, potentially exacerbating market movements. Bikhchandani et al. (1992) argue that social learning can often morph into herding behavior, especially when it involves complex decisions or when the environment is highly uncertain. This can lead to significant market implications, including bubbles and crashes, as decisions based on others' actions compound over time. Table 1 provide an overview of the types of herding and their respective causes, along with key references.

The significant influence of non-fundamental factors on perception alignment is underscored by Cui et al. (2019) and Indars et al. (2019). Cui et al. (2019) found that alignment among closed-end fund investors intensifies in response to market uncertainties and is often associated with the funds' trading discounts, suggesting that investor behaviors are influenced more by noise than by fundamental analysis. Indars et al. (2019) also note that investors on the Moscow Exchange align their actions in response to non-fundamental triggers, especially during volatile markets. This supports the concept that investor alignment can manifest independently of fundamental market shifts. Our research examines how the intensity of perception alignment relates to the level of information loss within the markets, particularly during periods of heightened uncertainty or significant economic announcements.

2. Information framework

Divergence measures from information theory provide a robust framework to quantify perception alignment among investors. By measuring the divergence or similarity between probability distributions of forecast errors or returns, we can infer the degree of alignment in investor behaviors.

2.1. Divergence measures

Divergence measures allow us to analyze the degree to which individual forecasts or investor behaviors align with a collective or theoretical benchmark. By examining the similarity or divergence between probability distributions associated with forecast errors, we can identify the conditions under which investor perceptions tend to converge or diverge, significantly impacting market stability and efficiency.

2.1.1. Kullback–Leibler divergence

The Kullback–Leibler divergence (KLD) quantifies the divergence between two probability distributions. Given a series of independently and identically distributed (i.i.d.) forecast errors $\{e\}$, we define their PDF as $f_i(e)$, and the PDF of the theoretically perfect forecast errors as $f^*(e)$. The divergence from $f_i(e)$ to $f^*(e)$, measured using KLD, is defined as

$$\mathcal{D}_{KL}(f_i; f^*) = \mathbb{E}_{f_i}\left(\log \frac{f_i(e)}{f^*(e)}\right) = \int_{-\infty}^{\infty} f_i(e) \log \frac{f_i(e)}{f^*(e)}\, de, \tag{1}$$

where $\mathcal{D}_{KL}(f_i; f^*) \geq 0$. Equality holds if and only if $f_i(e) = f^*(e)$, implying no divergence between the observed and ideal distributions (Kullback, 1959; Kullback & Leibler, 1951). This measure is asymmetric, meaning that $\mathcal{D}_{KL}(f_i; f^*) \neq \mathcal{D}_{KL}(f^*; f_i)$ which highlights its utility in distinguishing the directionality of information loss.

The use of KLD not only quantifies how far an individual's perceptions deviate from an ideal or collective benchmark but also provides a metric known as mutual information (MI), which can be derived from KLD to assess the overall information shared between the distributions:

$$\mathcal{M}(e; e^*) := \mathcal{D}_{KL}(f(e, e^*); f(e)f(e^*)) = \int_{-\infty}^{\infty} f(e, e^*) \log \frac{f(e, e^*)}{f(e)f(e^*)}\, de, \tag{2}$$

where $f(e, e^*)$ is the joint PDF of observed and perfect forecast errors. We will show how evaluating this divergence measure allows us to analyze perception alignment due to shifts in market dynamics driven by external news, policy changes, or emerging economic trends.

2.1.2. Jensen–Shannon divergence

The Jensen–Shannon divergence (JSD) is a symmetrized and smoothed version of the KLD utilized to measure the similarity between two probability distributions. This divergence is particularly valuable in financial analysis due to its symmetric property and boundedness. The JSD is calculated by first defining the mixture distribution $M(e)$ as

$$M(e) = \frac{1}{2}(f_i(e) + f^*(e)). \tag{3}$$

The divergence between $f_i(e)$ and $f^*(e)$ using JSD is then expressed as

$$\mathcal{D}_{JS}(f; f^*) = \frac{1}{2}\mathcal{D}_{KL}(f_i; M) + \frac{1}{2}\mathcal{D}_{KL}(f^*; M). \tag{4}$$

JSD offers several key properties. First, $\mathcal{D}_{JS}(f_i; f^*) = \mathcal{D}_{JS}(f^*; f_i)$, ensuring the measure is independent of the order of distributions. Also, $\mathcal{D}_{JS}(f_i; f^*)$ is always bounded between 0 and $\log(2)$, with 0 indicating identical distributions, and $\log(2)$ the maximum divergence when distributions do not overlap. The square root of $\mathcal{D}_{JS}$ serves as a metric, fulfilling the triangle inequality and providing a useful distance measure between distributions. For discussions on metric measures and their implications in inference and also applications of metric and non-metric divergence measures in econometrics and finance, refer to Maasoumi and Racine (2008), Racine and Maasoumi (2007), and Maasoumi and Racine (2016).

2.1.3. Rényi divergence

Rényi divergence (RD) incorporates a parameter α, enhancing the sensitivity of the measure to differences in probability distributions. This flexibility makes it useful in scenarios where different aspects of distributional divergence need emphasis. The RD of order α from $f_i(e)$ to $f(e^*)$ is defined as

$$\mathcal{D}_{\alpha}(f_i; f^*) = \frac{1}{\alpha - 1} \log \int_{-\infty}^{\infty} f_i(e)^{\alpha} f^*(e)^{1-\alpha}\, de, \tag{5}$$

where $\alpha \neq 1$. As α approaches 1, RD converges to KLD, highlighted by the limit:

$$\lim_{\alpha \to 1} \mathcal{D}_{\alpha}(f_i; f^*) = \mathcal{D}_{KL}(f_i; f^*). \tag{6}$$

Rényi divergence is defined for all $\alpha > 0$ and satisfies the non-negativity property, $\mathcal{D}_{\alpha}(f_i; f^*) \geq 0$, with equality if and only if $f_i = f^*$, indicating no divergence when the distributions are identical. Moreover, $\mathcal{D}_{\alpha}(f_i; f^*)$ is non-decreasing as a function of α, which accentuates differences particularly in regions where the distributions f_i and f^* diverge significantly. In the limit as $\alpha \to \infty$, Rényi divergence approximates the logarithm of the essential supremum ratio of the probability densities:

$$\lim_{\alpha \to \infty} \mathcal{D}_{\alpha}(f_i; f^*) = \log \sup \left\{ \frac{f_i(e)}{f^*(e)} : e \in \text{supp}(f_i) \cap \text{supp}(f^*) \right\}, \tag{7}$$

where $\text{supp}(f)$ denotes the support of the distribution f. This expression emphasizes the maximum ratio of the probabilities in regions where f_i is significantly greater than f^*, highlighting the extremes of the distribution.

2.1.4. f-divergence

The f-divergence is a broad class of statistical divergences that measures the difference between two probability distributions using a convex function. This family of divergences provides a flexible framework for analyzing and comparing distributional discrepancies based on various aspects. The general form of f-divergence from $f_i(e)$ to $f(e^*)$ is expressed as

$$\mathcal{D}_f(f_i; f^*) = \int_{-\infty}^{\infty} f_i(e^*) f\left(\frac{f_i(e)}{f(e^*)}\right) de, \tag{8}$$

Table 2
Summary of divergence measures.

Name	Definition	Key advantage
Kullback–Leibler $\mathcal{D}_{KL}(f_i; f^*)$	$\mathbb{E}_{f_i}\left(\log \frac{f_i(e)}{f^*(e)}\right)$	Sensitive to the differences between distributions, highlights information loss
Jensen–Shannon $\mathcal{D}_{JS}(f_i; f^*)$	$\frac{1}{2}\mathcal{D}_{KL}(f_i; M) + \frac{1}{2}\mathcal{D}_{KL}(f^*; M)$	Symmetric and bounded, provides a metric distance
Rényi $\mathcal{D}_\alpha(f_i; f^*)$	$\frac{1}{\alpha-1}\log\int f_i(e)^\alpha f^*(e)^{1-\alpha}\,\mathrm{d}e$	Parametrically adjustable sensitivity to distributional differences
f-divergence $\mathcal{D}_f(f_i; f^*)$	$\int f_i(e^*) f\left(\frac{f_i(e)}{f^*(e)}\right)\mathrm{d}e$	Adaptable to diverse analytical contexts, assessment of distributional discrepancies

where f_i is a convex function satisfying $f(1) = 0$. This setup ensures the divergence is non-negative, achieving zero specifically when $f_i(e) = f(e^*)$. The f-divergence is endowed with several properties: $\mathcal{D}_f(f_i; f^*) \geq 0$ for any convex function f_i, equating to zero only if $f_i = f^*$. The measure is convex regarding the pair of probability distributions. Different choices of the function f_i yield various known divergence measures: KLD with $f(t) = t\log t$, total variation distance using $f(t) = \frac{1}{2}|t-1|$, Hellinger distance via $f(t) = (\sqrt{t}-1)^2$, and Chi-squared divergence for $f(t) = (t-1)^2$.

These divergence measures are useful in quantifying perception alignment within financial markets. Among them, we focus on KLD for its sensitivity to differences between probability distributions, which is highly effective in identifying subtle shifts in investor behavior that may signal emerging trends or shifts in market sentiment, especially during extreme events (Ardakani, 2023a). KLD's asymmetry is particularly advantageous, allowing analysts to discern the direction of divergence—whether individual investor perceptions are converging towards or diverging from the market consensus or an idealized model. This feature is important in studies where the direction of information flow is significant (Ardakani, 2024), as it quantifies the information loss when one distribution substitutes for another, rather than merely indicating the existence of a difference (Ardakani, 2023b; Soofi, 1994; Soofi & Retzer, 2002).

While JSD offers a symmetrical and bounded alternative, it lacks the granularity of KLD in contexts where precise assessment of directional information flow is required. KLD's utility is not diminished by its non-metric nature; rather, it is enhanced in financial applications where understanding the directionality of information is critical. In some applications, the integration of KLD with metric divergences like JSD provides a robust methodological framework, combining the strengths of both measures to offer a comprehensive analysis of financial data distributions (Golan & Maasoumi, 2008; Gospodinov & Maasoumi, 2021). Moreover, KLD's ability to emphasize scenarios where one distribution significantly diverges from another is invaluable in financial markets characterized by risk and uncertainty. This divergence measure thus serves not only as a tool for comparison but also as a diagnostic instrument that can detect and quantify significant deviations in investor behavior and market dynamics. The properties and applications of divergence measures, including KLD and JSD, are extensively discussed in the literature, providing valuable insights into their utility in econometrics and finance (Ardakani et al., 2021; Beheshti et al., 2019; Maasoumi & Wang, 2019; Racine & Maasoumi, 2007). Table 2 provides a summary of various divergence measures used in financial analysis, each characterized by mathematical properties and applications.

2.2. Information loss

Perception alignment can extend beyond simple information sharing among informed investors. It can also occur in environments where investors, lacking substantial private information, choose to mimic the actions of others based on observable market behaviors—a process in which the convergence of actions does not necessarily stem from shared information but rather from a common reaction to public signals or observed actions (Hirshleifer et al., 1994). Perception alignment can also arise when investors with private information choose not to act on it because of the perceived costs of deviating from the consensus. This aligns with models of strategic behavior where individuals prioritize remaining inconspicuous within the market to avoid potential losses or reputational damage and leads to a convergence of observable behaviors that might mask underlying information diversity (Carlin et al., 2014).

Perception alignment is influenced by both exogenous and endogenous factors. Exogenously, market-wide news or regulatory changes can prompt a uniform update in beliefs across a wide array of investors, leading to temporary spikes in alignment. Endogenously, the continuous process of learning and belief updating, where investors refine their predictions based on new data and outcomes, can cause perceptions to either converge or diverge over time. Literature on trader disagreement and investor learning suggests that the degree of alignment is closely linked to the quality and ambiguity of available information. When high-quality, clear information is scarce, perceptions may diverge; conversely, the release of significant, clear-cut news can lead to rapid alignment (Carlin et al., 2014).

The effect of perception alignment driven by incoming signals does not necessarily lead to a degradation of informational value. When the incoming information is less noisy than the private information previously held by investors, this alignment can improve the overall utility of information within the market. This complicates the interpretation of shifts within forecast error distributions because convergence in investor behavior and forecasts may not diminish informational diversity but could instead optimize the utilization of available information. We employ the KLD to evaluate the effectiveness of how information is incorporated within market behaviors. A decrease in KLD might reflect a loss of diverse insights or an effective integration of superior information. The nature of the information influences how changes in KLD are interpreted. Perception alignment is defined as the statistical similarity between investors' beliefs about future returns. Under assumptions of 'information symmetry,' where all investors are equally informed about public data, though they may possess unique private information and 'forecast error independence,' with independently and identically distributed errors, we show increased perception alignment could lead to more significant information loss due to the standardization of forecast errors.

Definition 1. Let R_{t+1} denote the return of an asset at time $t+1$, and $\mathcal{I}_i$ represent the information set available to investor i at time t. Each investor forms beliefs about future returns based on their information set, denoted as $\mathcal{P}_i(R_{t+1}|\mathcal{I}_i)$. We define perception alignment between two investors i and j as the statistical similarity between their beliefs:

$$\mathcal{A}(\mathcal{P}_i, \mathcal{P}_j) = \mathcal{D}_{KL}(\mathcal{P}_i; \mathcal{P}_j), \tag{9}$$

where $\mathcal{D}_{KL}$ represents the Kullback–Leibler divergence. A lower value of $\mathcal{A}(\mathcal{P}_i, \mathcal{P}_j)$ indicates higher perception alignment, implying more homogeneous beliefs between the investors.

We postulate the following framework to structure our analysis:

Assumption 1 (*Information Symmetry*)**.** All investors share the same public information $\mathcal{I}_{\text{pub}}$ but may possess unique private information $\mathcal{I}_{\text{pri},i}$. Thus, each investor's complete information set is $\mathcal{I}_i = \mathcal{I}_{\text{pub}} \cup \mathcal{I}_{\text{pri},i}$.

Assumption 2 (*Forecast Error Independence*)**.** Forecast errors, $\{e_t\}$, are assumed to be independently and identically distributed (i.i.d.) across all time periods and investors.

Proposition 1. *Under Assumptions 1 and 2, an increase in perception alignment correlates with an increase in information loss. Specifically, if $\mathcal{A}(\mathcal{P}_i, \mathcal{P}_j)$ decreases, implying more similar beliefs, then $\mathcal{D}_{KL}(f(e); f(e^*))$ increases, signifying a loss of information diversity.*

Proof. Per the Definition 1, lower values of $\mathcal{D}_{KL}(\mathcal{P}_i; \mathcal{P}_j)$ indicate greater alignment of beliefs. Under Assumption 1, as beliefs $\mathcal{P}_i$ and $\mathcal{P}_j$ converge, so do the corresponding forecasts, yielding more identical forecast errors e_t. Given Assumption 2, this homogeneity in e_t reduces the diversity within the distribution of forecast errors $f_i(e)$. According to properties of the Kullback–Leibler divergence, this reduction in the variability of $f_i(e)$ leads to an increase in $\mathcal{D}_{KL}(f_i(e); f(e^*))$, which measures the divergence from $f_i(e)$ to an ideal distribution $f_i(e^*)$. Consequently, an increase in perception alignment results in greater information loss, as indicated by a rise in $\mathcal{D}_{KL}(f_i(e); f(e^*))$.

Example 1. Consider a scenario involving two investors, Investor A and Investor B, who engage in forecasting the price movements of a particular asset. For simplicity, their forecasts are binary predictions of whether the price of the asset will increase (denoted by "+") or decrease (denoted by "−"). Initially, both investors have access to the same public information, denoted by $\mathcal{I}_{\text{pub}}$, but they possess distinct private information, $\mathcal{I}_{\text{pri},A}$ and $\mathcal{I}_{\text{pri},B}$, leading to different forecasts:

$$\text{Investor A:} \quad +,+,-,+,-,+,-,+$$
$$\text{Investor B:} \quad -,+,-,-,+,-,+,-$$

These differences in forecasts indicate a significant divergence in their perceptions. We quantify the perception alignment, $\mathcal{A}(\mathcal{P}_A, \mathcal{P}_B)$, using the Kullback–Leibler divergence between their beliefs, which is initially high, reflecting substantial differences.

Assume now that an event occurs which significantly aligns their private information. The event could be a new macroeconomic report, a market-wide announcement, or any information that significantly impacts their asset-related beliefs. After this event, their updated forecasts might look as follows, reflecting a new consensus:

$$\text{Investor A:} \quad +,+,-,-,+,-,+,-$$
$$\text{Investor B:} \quad +,+,-,-,+,-,+,-$$

In this updated scenario, both investors have identical forecasts, demonstrating a complete alignment of their perceptions. Consequently, the Kullback–Leibler divergence between their beliefs, $\mathcal{A}(\mathcal{P}_A, \mathcal{P}_B)$, now approaches zero, indicating a maximal perception alignment under the given assumptions.

Proposition 2. *Given the assumptions of information symmetry and independent forecast errors, the Kullback–Leibler divergence, $\mathcal{D}_{KL}(f_i(e); f(e^*))$, serves as a robust indicator of the level of perception alignment among investors.*

Proof. Under Assumption 1, when perception alignment increases, it implies a reduction in $\mathcal{A}(\mathcal{P}_i, \mathcal{P}_j)$. This reduction signifies that the forecasts, and therefore the forecast errors, between investors become increasingly similar. Such similarity enhances the homogeneity of the error distribution $f_i(e)$, making it converge towards a delta function centered around the perfect forecast error, thus reducing the entropy of $f_i(e)$. As $f_i(e)$ becomes more like $f(e^*)$, $\mathcal{D}_{KL}(f_i(e); f(e^*))$ decreases. This decrease in divergence indicates an increase in perception alignment among investors, as the forecasts become more synchronized and less diverse.

Example 2. The use of the KLD measure in quantifying the information loss under the perception alignment hypothesis is illustrated using the following Monte Carlo examples. The Monte Carlo simulations are conducted using the R statistical package. Let e be nonnegative forecast errors, where $\log(e)$ is normally distributed, $\log(e) \sim \mathcal{N}(0, \sigma^2)$, and hence e is lognormally distributed. The PDF and cumulative distribution function (CDF) of the standard lognormal error density with location and scale parameters 0 and 1 and shape parameter θ can be written as

$$f(e) = \frac{1}{e\theta\sqrt{2\pi}} e^{-(\log e)^2/2\theta^2} \tag{10}$$

$$F(e) = \Phi(\frac{\log e}{\theta}), \tag{11}$$

where $\theta > 0$ and $\Phi(\cdot)$ is the normal distribution CDF.

We simulate a sequence of forecast errors from the lognormal distribution with $\theta = .6, .7, .8, .9$. The PDFs and empirical CDFs of the simulated data are shown in the left panel of Fig. 1. The error density with $\theta = .6$ has a lighter tailed than the other error densities. Table 3 summarizes $\mathcal{D}_{KL}(f_i; f^*)$ measures between the simulated and ideal forecast error densities. The simulation results indicate a decline in $\mathcal{D}_{KL}(f_i; f^*)$ as θ increases from .6 to .8. This example illustrates more information is gained when using ideal forecast errors compared to lognormal densities with smaller shape parameters. This can be interpreted as reducing the discrepancy between the observed error distribution and the perfect error distribution. The lower the KLD, the more the actual errors resemble perfect ones.

The second Monte Carlo study considers heavy-tailed data. The previous literature has shown that heavy-tailed distributions are better fits for modeling asset returns (Ardakani, 2022; Cont, 2001; Gua, 2017). We simulate from two heavy-tailed Pareto and Skewed t. The PDF and CDF of Pareto with shape parameter α can be written as

$$f(e) = \frac{\alpha}{e^{\alpha+1}} \tag{12}$$

and

$$F(e) = 1 - \frac{1}{e^{\alpha}}, \tag{13}$$

where $\alpha \geq 1$. The middle panel in Fig. 1 plots the PDFs and empirical CDFs of the Pareto distributions with $\alpha = 2.5, 3, 3.5, 4$. Pareto with $\alpha = 4$ is more concentrated than the other three. Table 3 shows that for Pareto $\mathcal{D}_{KL}(f_i; f^*)$ is decreasing in α. The expected value and variance are not defined for Pareto with $\alpha \leq 1$ and $\alpha \leq 2$. Another heavy-tailed density used in asset pricing is Skewed t introduced by Hansen (1994) and has the best goodness of fit to model financial asset returns (Gua, 2017). The Skewed t PDF with the skewing parameter γ can be written as

$$\begin{cases} f(e) = \frac{2}{\gamma + \frac{1}{\gamma}} g(\gamma e) & \text{for } e < 0 \\ f(e) = \frac{2}{\gamma + \frac{1}{\gamma}} g(\frac{e}{\gamma}) & \text{for } e \geq 0, \end{cases} \tag{14}$$

where $g(\cdot)$ is the PDF of the t distribution. The third panel in Fig. 1 plots the PDFs and empirical CDFs of Skewed t distributions with $\gamma = 1.5, 2, 2.5, 3$. Skewed t with $\gamma = 3$ is the most heavy-tailed among the four densities and its CDF is ranked the lowest. The KLD values presented in Table 3 increase with the heaviness of the tails in the distribution, noticeable in the skewed t distribution. This increase in KLD from the empirical distributions to the ideal forecast distribution indicates a growing disparity as the tail heaviness increases, underscoring KLD's sensitivity to discrepancies in the tails of distributions. JSD provides a view by averaging the divergence to a central mixed distribution. The JSD values, also listed in Table 3, provide a complementary perspective to KLD, particularly useful in assessing the overall alignment of distributions without the directional bias in KLD. The directional sensitivity of KLD, which distinguishes how an empirical distribution either underestimates or overestimates the characteristics of the ideal distribution, is particularly highlighted. This is evident from the differing values of $\mathcal{D}_{KL}(f_i; f^*)$ and $\mathcal{D}_{KL}(f^*; f_i)$ for each type of distribution. Such directional information is invaluable for understanding whether the empirical distribution tends to produce forecasts that are consistently more conservative or more aggressive compared to the ideal distribution.

2.3. Application to high-frequency data

This framework can be employed to analyze high-frequency trading data and measure the extent of information loss when perception alignment drives trading activity. High-frequency data can reveal the underlying dynamics of the perception alignment. Our empirical analysis involves generating i.i.d forecast errors by modeling high-frequency data. An effective modeling approach was proposed by Bollerslev and Wright (2001), among others, who suggest capturing volatility dynamics by fitting an autoregressive model to high-frequency returns. They show this autoregressive model outperforms GARCH models when working with high-frequency data, providing more accurate and consistent results. Consequently, we utilize the standard autoregressive integrated moving average, or ARIMA(p, d, q), to model the high-frequency data.

The ARIMA(p, d, q) is defined as

$$(1 - L^d) r_t = c + \phi(L) r_t + \theta(L)\varepsilon_t, \tag{15}$$

where $\{r_t\}_{t=1}^T$ is a sequence of returns, L is the lag operator, $\{\varepsilon\}_{t=1}^T$ is a serially uncorrelated white noise sequence, and $\phi(\cdot)$ and $\theta(\cdot)$ are polynomials of order p and q. To select the optimal orders p, d, q, Hyndman and Khandakar (2008) provide an algorithm in which unit root tests, AIC minimization, and maximum likelihood estimation are used. The data are first tested for a unit root

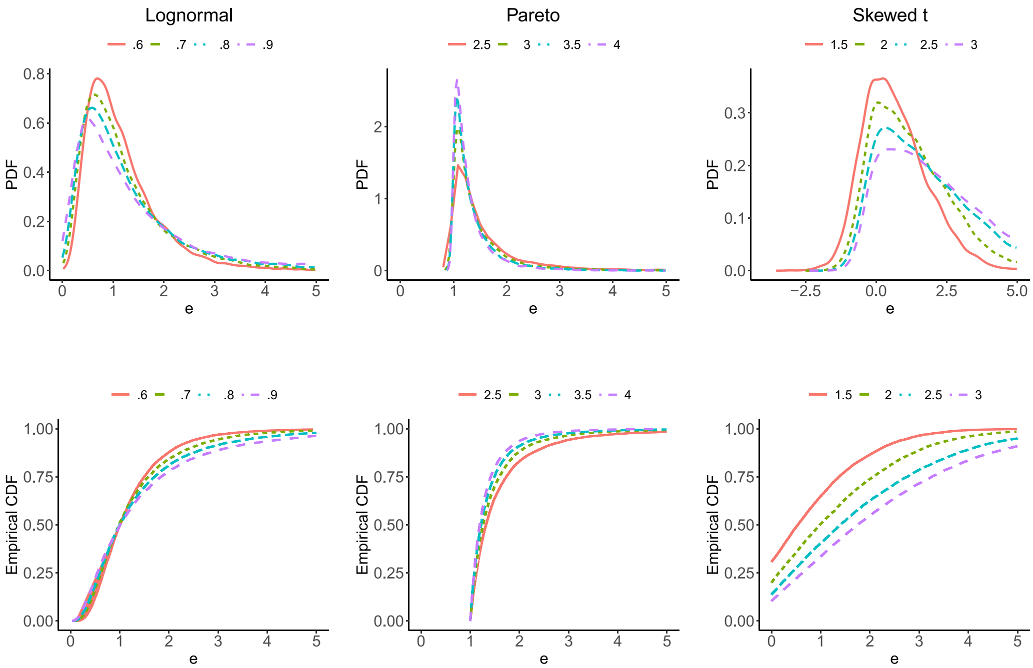

Fig. 1. PDFs and empirical CDFs of simulated forecast errors from lognormal distribution with $\theta = .6, .7, .8, .9$ (left panel), Pareto with $\alpha = 2.5, 3, 3.5, 4$ (middle panel), and Skewed t with $\gamma = 1.5, 2, 2.5, 3$ (right panel).

Table 3
Divergence measures for simulated data.

Distribution	$\mathcal{D}_{KL}(f_i; f^*)$	$\mathcal{D}_{KL}(f^*; f_i)$	$\mathcal{D}_{JS}(f^*; f_i)$
Lognormal			
.6	1.81	1.81	1.81
.7	0.74	0.46	0.60
.8	0.72	0.45	0.59
.9	0.73	0.45	0.59
Pareto			
2.5	0.75	0.50	0.62
3.0	0.71	0.46	0.59
3.5	0.67	0.44	0.56
4.0	0.66	0.42	0.54
Skewed t			
1.5	1.84	1.38	1.61
2.0	3.22	2.2	2.71
2.5	3.41	2.71	3.06
3.0	4.32	3.53	3.93

$\mathcal{D}_{KL}(f_i; f^*)$ quantifies the Kullback–Leibler divergence from the empirical distribution to the theoretical model, $\mathcal{D}_{KL}(f^*; f_i)$ represents the reverse divergence, and $\mathcal{D}_{JS}(f^*; f_i)$ reflects the Jensen–Shannon divergence.

based on successive KPSS (Kwiatkowski et al., 1992) to find the integrated order d. Then, the autoregressive and moving average orders p, q are selected via $AIC = -2\log(\mathcal{L}) + 2(p+q)$, where $\mathcal{L}$ is the maximized likelihood.

Once the optimal ARIMA model is selected and fit, one-step-ahead forecasts are computed through a rolling forecasting scheme. These forecasts are then scaled by the standard deviation of forecast errors, resulting in our desired errors. These are used to calculate the KLD between the optimal and ideal error densities, effectively quantifying the information gain when the optimal error density is utilized instead of the ideal one. As $\mathcal{D}_{KL}(f_i; f^*)$ reduces, it signifies a decline in information gain. This reflects the impact of perception alignment in high-frequency market data.

In practice, the approach involves two main steps: (1) modeling the high-frequency data and estimating the out-of-sample forecast error PDF, and (2) computing the KLD between the optimal forecast error PDF and the ideal counterpart, thereby quantifying the loss of information induced by aligning investors' expectations.

2.4. Herd behavior conditional on information flow

Understanding the conditions that prompt investors to engage in herding allows us better analyze market dynamics, especially during times of high volatility or pronounced information asymmetry. Perception alignment leads to spurious herding causing markets to move in unison without a deliberate decision to mimic others' actions. Such herding results from the homogeneous processing of information across the market. As investors react to public news or global events, their perceptions align and drive a uniformity in behavior that displays as spurious herding. This uniformity is a form of information loss since it diminishes the diversity of individual decisions.

The Cross-Sectional Absolute Deviation (CSAD), when integrated with measures of information asymmetry can provide a framework to evaluate how investor reactions vary with the flow and clarity of information. This combination allows us to assess the extent of herding and the quality of information driving such behaviors. Drawing from the insights of Chang et al. (2000) and Galarioitis et al. (2015), we discuss the conceptual use of CSAD combined with KLD to analyze herding behavior under different states of information asymmetry. Following Chang et al. (2000), CSAD is used to measure deviations of individual asset returns from the average market return:

$$\mathrm{CSAD}_t = \frac{1}{N}\sum_{i=1}^{N} \left| R_{i,t} - R_{m,t} \right|, \tag{16}$$

where $R_{i,t}$ is the return of asset i at time t, and $R_{m,t}$ is the average market return at that time. To adjust returns for expected market behavior using the Capital Asset Pricing Model, we can define

$$\mathrm{E}(R_{i,t}) = R_f + \beta_i (R_{m,t} - R_f), \tag{17}$$

where R_f is the risk-free rate, and β_i is the beta of asset i. Adjusted CSAD is then

$$\mathrm{CSAD}_t^A = \frac{1}{N}\sum_{i=1}^{N} \left| R_{i,t} - \mathbb{E}(R_{i,t}) \right|. \tag{18}$$

The dynamic relationship between CSAD and information asymmetry can be modeled using KLD as

$$\mathrm{CSAD}_{t|\mathcal{D}_{KL}} = f(\mathcal{D}_{KL}(f_t; f^*)), \tag{19}$$

suggesting that CSAD is conditioned on the current state of information asymmetry as quantified by KLD. A regression model can analyze the impact:

$$\mathrm{CSAD}_{t|\mathcal{D}_{KL}} = \beta_0 + \beta_1 \mathcal{D}_{KL} + \epsilon_t, \tag{20}$$

where β_1 tests the effect of information asymmetry on herding behavior.

3. Empirical studies

This section empirically examines how perception alignment is exemplified during the COVID-19 pandemic. This analysis is anchored on the behavior of the volatility index during this period. This provides a unique lens through which to view the collective response of investors to unfolding global events. By leveraging minute-by-minute VIX data, we can trace rapid shifts in market sentiment and the corresponding alignment of investor perceptions under extreme events. Following the examination of the VIX, we extend our empirical analysis to the Australian Securities Exchange, focusing on the S&P/ASX 200 index during the sharp market sell-off in early March 2020.

3.1. The volatility index during the pandemic

At the onset of the COVID-19 pandemic, the CBOE volatility index reached new heights last experienced during the 2008 financial crisis. This significant increase was notably influenced by the World Health Organization's announcement declaring COVID-19 a pandemic. Such an event provides an empirical context to examine how investor perceptions align in response to global health crises and their impact on financial markets. The VIX, which is derived from S&P 500 index options, measures market risk and investors' sentiments by capturing the market's expectation of 30-day forward-looking volatility. This measure assesses how investors' perceptions of future asset returns align following major announcements or global events. We utilize minute-by-minute VIX data accessed through the Bloomberg Terminal. This approach allows us to track the rapid changes in market sentiment and examine the extent to which investors' perceptions converge in response to new information. Such an analysis can offer insights into the behavioral dynamics of financial markets under stress and highlight the role of significant public announcements in shaping market behavior.

On each trading day, high-frequency VIX is available during regular and extended trading hours between 3:15 a.m. and 4:15 p.m. ET. In a day and within the 13 trading hours, 764 one-minute observations are provided. Our sample period ranges from January 22, 2020, at 4:24 a.m. to April 24, 2020, at 4:14 p.m., including 48,782 observations. We observed jumps in high-frequency VIX around when the WHO declared the pandemic as a public health emergency. The VIX jump was highest on March 9, 2020, at 9:54 a.m., when VIX soared 15.42 points from 41.94 at 9:53 a.m. to 57.36 at 9:54. We consider this time as a breakpoint and choose

Table 4
VIX summary statistics.

Series	μ_n	s	γ	κ
Entire sample				
v_t	37.36	19.48	0.34	2.02
r_t	0.00	0.31	−0.01	5.64
r_t^2	0.10	0.20	4.04	22.69
Pre-jump period				
v_t	21.25	9.60	1.35	3.60
r_t	0.00	0.31	0.01	5.81
r_t^2	0.10	0.21	4.01	22.07
Post-jump period				
v_t	53.47	12.14	0.61	2.29
r_t	0.00	0.31	−0.04	5.44
r_t^2	0.09	0.20	4.06	23.19

$\mu_n, s^2, \gamma, \kappa$ are the first four moments in order. v_t is the high-frequency VIX, and r_t and r_t^2 are return and return-squared.

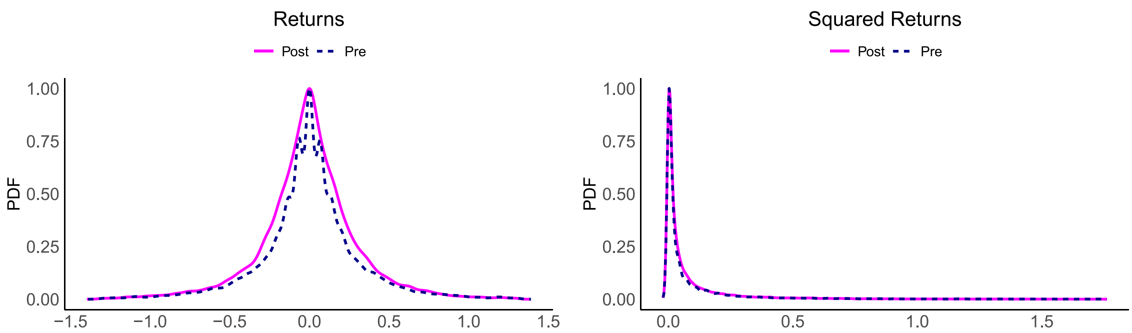

Fig. 2. The PDFs of the high-frequency VIX return and return-squared for the pre- and post-jump subsamples.

the same sample size for the pre- and post-jump subsamples, where each includes 24,391 observations. As a robustness check, we also consider other samples based on various jumps starting from February 24 at 3:15 a.m. with jump size 5.16. The returns r_t are calculated by the difference log in the price index v_t, $r_t = 100\log(v_t/v_{t-1})$. Returns are used at the 99.5th percentile, excluding the values below -1.32 (263 observations) and above 1.32 (253 observations).

Table 4 presents summary statistics for the high-frequency VIX data (v_t), along with its return (r_t) and squared return (r_t^2), segmented into entire, pre-jump, and post-jump samples. The table includes the first four moments: mean (μ_n), variance (s^2), skewness (γ), and kurtosis (κ), providing an overview of the data distribution. Notably, both v_t and r_t^2 exhibit right-skewness across all periods, suggesting a tendency for larger upward movements, which is characteristic of volatility indices during turbulent market conditions. The return densities (r_t) are symmetric, indicating no directional bias in price movements, while the pronounced kurtosis in r_t^2 highlights the presence of heavy tails, typical of financial time series data and indicative of potential outlier effects or abrupt market shifts. The contrast in variance and kurtosis before and after the jump underscores the significant impact of market events on volatility perceptions, which is crucial for understanding investor behavior and market dynamics during periods of stress.

Fig. 2 plots the PDFs of high-frequency VIX return and return-squared for the two pre- and post-jump subsamples. The left panel shows that the return densities are symmetric and centered around zero. In contrast, return-squared densities are right-skewed and heavy-tailed, confirming the results in Table 4. Neither PDFs in Fig. 2 nor summary measures in Table 4 provide information about the presence of perception alignment during the pandemic. We apply the framework described in Section 2 to examine these impacts. We first compute the out-of-sample forecast errors and then find the divergence between the optimal and ideal forecast error densities before and during the pandemic.

The literature provides extensive evidence of perception alignment in financial markets (Dalko et al., 2016; Hansen et al., 2004; Jiang et al., 2005; Khwaja & Mian, 2005). Building upon this foundation, we apply the proposed framework for quantifying the degree of perception alignment and examining its dynamics during the COVID-19 pandemic. We compute out-of-sample forecast errors using an ARIMA model, as outlined in (15), to measure the extent of alignment. We then assess the information loss in the market during the pandemic period, utilizing KLD and ideal forecast models to capture the impact of these collective behaviors.

The results of ARIMA models for high-frequency return-squared are summarized in Table 5. Based on the algorithm introduced by Hyndman and Khandakar (2008), the optimal models for the entire, pre-, and post-jump periods are selected as ARIMA$(2,1,3)$, ARIMA$(0,1,2)$, and ARIMA$(3,1,2)$. The optimal models are used for computing out-of-sample forecast errors on a rolling forecasting scheme. The rolling window includes 23,618 observations for the pre-jump period, and out-of-sample forecasting starts on March 6, 2020, at 3:15 a.m. For the post-jump period, the window is 23,665, and forecasting starts from April 24, 2020, at 3:51. The

Table 5
The results of ARIMA models for VIX return-squared.

Coefficient	Entire ARIMA(2,1,3)	Pre ARIMA(0,1,2)	Post ARIMA(3,1,2)
ϕ_1	0.08		0.30
	(0.04)		(0.01)
ϕ_2	0.78		0.03
	(0.05)		(.01)
ϕ_3			0.01
			(0.01)
θ_1	−1.01	−0.91	−0.59
	(0.04)	(0.01)	(0.10)
θ_2	−0.72	−0.04	−0.35
	(0.08)	(0.01)	(0.10)
θ_3	0.73		
	(0.04)		
$\log \mathcal{L}$	12 180	5567	6574
AIC	−24 349	−11 128	−13 137
RMSE	0.188	0.192	0.184

ϕ_i and θ_i are the autoregressive and moving average coefficients.
$\log \mathcal{L}$ is the log-likelihood, and RMSE is the root mean squared error. 'Pre' refers to the period before the first jump prior to the WHO announcement of the pandemic, and 'post' refers to the period during the COVID-19 pandemic.

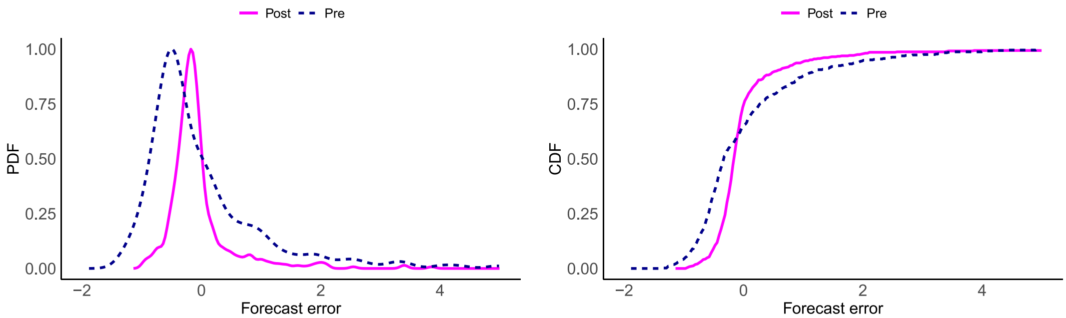

Fig. 3. PDFs and empirical CDFs of scaled out-of-sample forecast errors before and during the COVID-19 crisis.

out-of-sample forecast errors for both pre- and post-periods include 492 observations. The results are robust to alternative window width selection.

Fig. 3 presents PDFs and empirical CDFs of scaled out-of-sample forecast errors before and during the COVID-19 crisis. Although the PDFs of return-squared shown in Fig. 2 are indistinguishable across the sample periods, Fig. 3 clearly shows the distinction between PDFs and CDFs of the forecast errors for the two periods. The error CDF of the post-pandemic is closer to the ideal forecast error CDF. Also, the error PDF of the post-pandemic is more concentrated around zero with a lighter tail. We quantify the divergence between the error densities using the KLD. Further discussion on ranking forecasts based on distances between the forecast error CDF and ideal forecast error CDF can be found in Ardakani et al. (2018) and Diebold and Shin (2017).

Table 6 presents the divergence measures for high-frequency VIX before and during the COVID-19 pandemic, employing Kullback–Leibler and Jensen–Shannon divergences. These measures quantify the discrepancy and symmetrical relationship between the empirical distribution of VIX values and a theoretical ideal during significant market shifts. $\mathcal{D}_{KL}(f_i; f^*)$ measures the information loss when transitioning from an empirical distribution to a theoretical ideal, while $\mathcal{D}_{KL}(f^*; f_i)$ assesses the divergence from the ideal to the empirical distribution, providing insight into the extent of overestimation or underestimation of the market's perceived risk. Notably, both $\mathcal{D}_{KL}(f_i; f^*)$ and $\mathcal{D}_{KL}(f^*; f_i)$ decreased significantly from the pre-pandemic to the post-pandemic period, suggesting a reduction in the informational asymmetry between market perceptions and the ideal state. This reduction implies an increased alignment in investor perceptions as the market adapted to the new reality imposed by the pandemic. The $\mathcal{D}_{JS}(f_i; f^*)$, a symmetrized measure, provides a balanced view of the divergence, averaging the discrepancies from both directions. The decrease in this measure from 1.331 pre-pandemic to 0.686 post-pandemic reflects a more coherent market perception alignment towards the VIX's theoretical ideal. This observation underscores the impact of global events on converging investor sentiments, amplifying perception alignment effects during times of heightened uncertainty and risk.

Andersen et al. (2015) highlight that deviations in the VIX index from actual market volatility may occur due to the inclusion of illiquid options. Similarly, Saha et al. (2019) demonstrate that variations in daily VIX levels are predominantly driven by market fundamentals. Under the framework of perception alignment, the expectations of traders regarding future prices shape the future price density. This alignment of perceptions influences the higher moments of the price density, reflecting the collective market sentiment about future volatility, which is manifested in the 30-day forecast of volatility derived from put and call options.

Table 6
Divergence measures for high-frequency VIX.

Period	$\mathcal{D}_{KL}(f_i; f^*)$	$\mathcal{D}_{KL}(f^*; f_i)$	$\mathcal{D}_{JS}(f^*; f_i)$
Pre-pandemic	1.398	1.263	1.331
Post-pandemic	0.885	0.487	0.686

$\mathcal{D}_{KL}(f_i; f^*)$ quantifies the Kullback–Leibler divergence from the observed forecast error distribution to the ideal forecast error density, reflecting the degree of information loss. $\mathcal{D}_{KL}(f^*; f_i)$ measures the divergence from the ideal to the empirical distribution, highlighting the extent of overestimation or underestimation in the perceived risk. $\mathcal{D}_{JS}(f^*; f_i)$ is the Jensen–Shannon divergence.

Table 7
A sensitivity analysis for VIX jumps before and during the pandemic in 2020.

Jump time	Size	Pre-pandemic		Post-pandemic	
		Model	$\mathcal{D}_{KL}(f_i; f^*)$	Model	$\mathcal{D}_{KL}(f_i; f^*)$
February 24, 3:15 am	5.16	ARIMA(1,1,1)	2.29	ARIMA(1,1,2)	0.87
March 12, 3:15 am	7.59	ARIMA(2,1,3)	1.85	ARIMA(3,1,1)	0.74
March 16, 9:48 am	18.52	ARIMA(0,1,2)	1.31	ARIMA(3,1,5)	0.73
March 17, 12:07 pm	6.25	ARIMA(2,1,3)	1.91	ARIMA(3,1,1)	0.72
March 18, 1:12 pm	5.56	ARIMA(0,1,2)	2.25	ARIMA(3,1,5)	1.88

'Size' represents the size of the jump. $\mathcal{D}_{KL}(f_i; f^*)$ is the Kullback–Leibler divergence from the observed forecast error distribution to the ideal forecast error density, reflecting the degree of information loss.

The certainty or uncertainty held by traders about future price movements can significantly impact the distribution's shape, effectively translating information asymmetries into observable market metrics. Additionally, activities in both spot and derivatives markets may be intertwined as traders might elevate spot prices while capitalizing on movements in the derivatives market. This behavior, although potentially manipulative, often escapes immediate regulatory scrutiny due to the jurisdictional differences between the entities overseeing these markets. Our analysis leverages high-frequency VIX data to account for these dynamics, exploring how collective expectations and individual strategies align to influence market indicators under the perception alignment hypothesis.

As a sensitivity analysis, we consider different jumps in high-frequency VIX sizes larger than five from February 1 through March 23, 2020. Table 7 presents the time when the jump occurred with its size. The smallest jump size is 5.16 on February 24 at 3:13 a.m., and the largest is 18.52 on March 16 at 9:48 a.m. The table also shows the optimal forecasting model for the pre- and post-jump periods, along with the corresponding $\mathcal{D}_{KL}(f; f^*)$ measures. For all jumps, $\mathcal{D}_{KL}(f; f^*)$ has declined in the post-jump period during the COVID-19 crisis. These results confirm the robustness of our main findings in Table 6.

3.2. *Australian security index*

The Australian Securities Exchange (ASX) is Australia's primary securities exchange, recognized globally among leading exchanges. The benchmark index of the ASX, the S&P/ASX 200, comprises shares from the 200 largest companies in Australia, representing the performance of large-cap Australian equities. Our analysis considers this index, particularly in response to the sharp sell-off observed in early March 2020, as noted by Housego (2020). This period is of interest as a potential case of rapid perception alignment among investors responding to global events and uncertainties. This shift in market dynamics, away from regular trading patterns, underscores the need to understand investor behavior during periods of significant market stress.

We implement the analytical framework described in Section 2 using daily data from the ASX, sourced from the Bloomberg Terminal. This dataset spans from January 2016 to October 2020, encompassing 1203 observations. The ASX's performance, illustrated in the first row of Fig. 4, shows a pronounced decline in index values alongside a notable increase in return volatility. Specifically, the ASX plummeted from 6216.21 on March 6, 2020, to 4546.03 on March 23, 2020—a substantial 1670.18-point drop. We segment the data into pre- and post-pandemic periods.

Table 8 gives the summary measures for the ASX values and returns across all samples. The minimum and maximum ASX values for the entire sample are 4546 and 7162, with a mean of 4546 and a standard deviation of 500. The return ranges from −10.2 to 6.76, with a mean of .01 and a standard deviation of 1.08. The average return drops and the standard deviation rises for the post-pandemic period. The second row in Fig. 4 plots the densities of pre- and post-pandemic samples. Density plots for returns remain similar for the two sample periods.

Table 9 presents the results of ARIMA models and the KLD measures for daily returns on the ASX. The chosen ARIMA models for the entire dataset, pre-pandemic, and post-pandemic periods are ARIMA(5,0,5), ARIMA(2,0,2), and ARIMA(1,0,3), respectively. The RMSE is lowest in the pre-pandemic period, indicating more precise forecasts, and highest in the post-pandemic period, reflecting greater volatility and prediction challenges during the pandemic. The KLD measures, which quantify the divergence from the empirical distribution to a theoretical ideal, decrease from 0.803 in the pre-pandemic period to 0.214 in the post-pandemic period. This reduction in KLD suggests a narrowing of the gap between observed market behaviors and the theoretical model, indicating more consistent investor behavior in the face of pandemic-induced uncertainty.

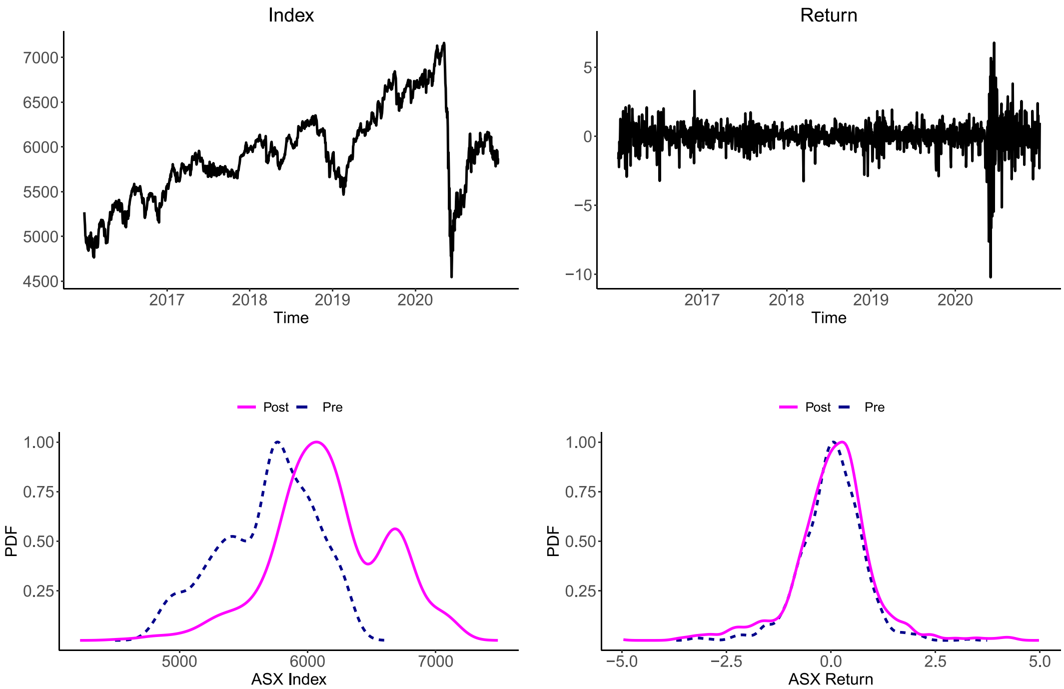

Fig. 4. Plots of the ASX values and returns along with the corresponding density plots.

Table 8
ASX summary measures.

Series	μ_n	s	γ	κ
Entire sample				
a_t	5903	500	0.17	2.73
r_t	0.01	1.08	−1.41	19.11
Pre-pandemic				
a_t	5687	368	−0.41	2.43
r_t	0.02	0.72	−0.38	5.34
Post-pandemic				
a_t	6167	442	−0.16	3.21
r_t	0	1.26	−1.47	17.26

$\mu_n, s^2, \gamma, \kappa$ are the first four moments in order. a_t is the daily S&P/ASX 200 index, and r_t are returns.

Table 9
The results of the ARIMA models with the KLD measures for ASX daily returns.

	Entire sample	Pre-pandemic	Post-pandemic
Model	ARIMA(5,0,5)	ARIMA(2,0,2)	ARIMA(1,0,3)
AIC	3521.73	1506.19	2251.45
MAPE	232.83	149.29	328.79
RMSE	1.03	0.71	1.21
$\log \mathcal{L}$	−1749.86	−748.09	−1120.72
$\mathcal{D}_{KL}(f_i; f^*)$	0.657	0.803	0.214

The AIC is the Akaike information criterion. The MAPE is the mean absolute percentage error. The RMSE is the root mean squared error, and $\log \mathcal{L}$ is the log-likelihood. $\mathcal{D}_{KL}(f_i; f^*)$ is the Kullback–Leibler divergence from the observed forecast error distribution to the ideal forecast error density, reflecting the degree of information loss.

4. Discussion

This paper studies perception alignment within financial markets and utilizes the COVID-19 crisis to examine the effects of global disruptions on financial systems. We analyze rapid changes in investor sentiment precipitated by public news dissemination and global events during this heightened uncertainty. This leads to information loss and influences market stability. This study quantifies how perceptions about future market prices shape price densities and contribute to market stability or instability by employing an information-theoretic framework and utilizing high-frequency data, particularly from the VIX. Our methodological approach builds on Clark (1973), Easley et al. (2012), and Mandelbrot and Taylor (1967), who have highlighted the significance of volume time and transaction-based pricing in decoding market behaviors. The integration of volume-based data allows for an understanding of how perception alignment influences market dynamics.

Our empirical study shows that during COVID-19, there was a noticeable increase in information loss as investor perceptions converged in response to news dissemination. This alignment was associated with market fluctuations. This finding highlights the market's sensitivity to external shocks. The analysis of high-frequency VIX reveals how rapid adjustments in investor perceptions can lead to substantial price movements. The impact of public news during the pandemic highlights its dual role. While essential for informed decision-making, it also causes significant shifts in market sentiment, sometimes based on speculative or incomplete information. The global nature of the pandemic and its impacts across different economic sectors further illustrate the interconnectedness of financial markets. The collective movement of global investors, often in response to synchronized policy actions, reflects a broader trend of global perception alignment.

This study extends conventional theories on market behavior by integrating perception alignment into the analysis of market dynamics during periods of crisis. It provides a framework for understanding how collective investor behaviors can destabilize markets or lead to rapid adjustments in market prices.

5. Concluding remarks

We employ divergence measures from information theory to quantitatively assess the extent of perception alignment among investors. Kullback–Leibler divergence, complemented by additional divergence measures, allows us to examine the alignment of individual investors' forecasts with the aggregate market sentiment. This approach is applied to evaluate the impacts of the pandemic on financial markets. We document substantial shifts in investor behavior in response to significant informational events by quantifying the divergence between empirical probability distributions of forecast errors and a theoretical benchmark. This framework captures either convergence of collective market perceptions or divergence in response to new information.

Future research can extend the current framework to include diverse markets and asset classes, such as bonds, commodities, and cryptocurrencies to study market dynamics across different sectors. We can also incorporate data analytics and machine learning techniques to detect and predict market manipulation and collective investment behaviors. An additional research direction is the integration of transaction-based pricing with high-frequency and volume-based data for developing models that reflect the underlying mechanics of market dynamics and provide a framework for examining how market sentiments and economic events influence price movements.

Declaration of competing interest

The authors have no conflicts of interest to declare that are relevant to the content of this article.

Acknowledgment

We thank the editor and the reviewers for their insightful comments, which have significantly enhanced this manuscript.

Data availability

Data will be made available on request.

References

Allen, F., & Gale, D. (1992). Stock-price manipulation. *The Review of Financial Studies*, *5*(3), 503–529.
Andersen, T. G., Bollerslev, T., Diebold, F. X., & Vega, C. (2003). Micro effects of macro announcements: Real-time price discovery in foreign exchange. *American Economic Review*, *93*(1), 38–62.
Andersen, T. G., Bollerslev, T., Diebold, F. X., & Vega, C. (2007). Real-time price discovery in global stock, bond and foreign exchange markets. *Journal of International Economics*, *73*(2), 251–277.
Andersen, T. G., Bondarenko, O., & Gonzalez-Perez, M. T. (2015). Exploring return dynamics via corridor implied volatility. *The Review of Financial Studies*, *28*(10), 2902–2945.
Ardakani, O. M. (2022). Option pricing with maximum entropy densities: The inclusion of higher-order moments. *Journal of Futures Markets*, *42*, 1821–1836.
Ardakani, O. M. (2023a). Capturing information in extreme events. *Economics Letters*, *231*, Article 111301.
Ardakani, O. M. (2023b). Coherent measure of portfolio risk. *Finance Research Letters*, *57*, Article 104222.
Ardakani, O. M. (2024). Portfolio optimization with transfer entropy constraints. *International Review of Financial Analysis*, *96*, Article 103644.
Ardakani, O., Asadi, M., Ebrahimi, N., & Soofi, E. (2021). Variants of mixtures: Information properties and applications. *Journal of the Iranian Statistical Society*, *20*(1), 27–59.
Ardakani, O. M., Ebrahimi, N., & Soofi, E. S. (2018). Ranking forecasts by stochastic error distance, information and reliability measures. *International Statistical Review*, *86*(3), 442–468.
Avery, C., & Zemsky, P. (1998). Multidimensional uncertainty and herd behavior in financial markets. *American Economic Review*, *88*(4), 724–748.
Babii, A., Ghysels, E., & Striaukas, J. (2022). Machine learning time series regressions with an application to nowcasting. *Journal of Business & Economic Statistics*, *40*(3), 1094–1106.

Baker, M., & Wurgler, J. (2007). Investor sentiment in the stock market. *Journal of Economic Perspectives*, *21*(2), 129–151.
Banerjee, A. V. (1992). A simple model of herd behavior. *Quarterly Journal of Economics*, *107*(3), 797–817.
Barber, B. M., Odean, T., & Zhu, N. (2006). Do noise traders move markets? In *SSRN electronic journal*, *EFA 2006 zurich meetings paper*.
Beheshti, N., Racine, J. S., & Soofi, E. S. (2019). Information measures of kernel estimation. *Econometric Reviews*, *38*(1), 47–68.
Bikhchandani, S., Hirshleifer, D., & Welch, I. (1992). A theory of fads, fashion, custom, and cultural change as informational cascades. *Journal of Political Economy*, *100*(5), 992–1026.
Blasco, N., & Ferreruela, S. (2008). Testing intentional herding in familiar stocks: an experiment in an international context. *Journal of Behavioral Finance*, *9*(2), 72–84.
Bohren, J. A. (2016). Informational herding with model misspecification. *Journal of Economic Theory*, *163*, 222–247.
Bollerslev, T., & Wright, J. H. (2001). High-frequency data, frequency domain inference, and volatility forecasting. *The Review of Economics and Statistics*, *83*(4), 596–602.
Bowe, M., & Domuta, D. (2004). Investor herding during financial crisis: A clinical study of the jakarta stock exchange. *Pacific-Basin Finance Journal*, *12*(4), 387–418.
Boyson, N. M. (2010). Implicit incentives and reputational herding by hedge fund managers. *Journal of Empirical Finance*, *17*(3), 283–299.
Caparrelli, F., D'Arcangelis, A. M., & Cassuto, A. (2004). Herding in the Italian stock market: A case of behavioral finance. *Journal of Behavioral Finance*, *5*(4), 222–230.
Carlin, B., Longstaff, F. A., & Matoba, K. (2014). Disagreement and asset prices. *Journal of Financial Economics*, *114*(2), 226–238.
Carvajal, A., & Elliott, J. E. (2009). *The challenge of enforcement in securities markets: Mission impossible?*: *MF Working Paper No. 09/168*, (p. 38).
Casoli, C., & Lucchetti, R. (2022). Permanent-transitory decomposition of cointegrated time series via dynamic factor models, with an application to commodity prices. 25 (2) 494–514.
Chacon, H. D., Kesici, E., & Najafirad, P. (2020). Improving financial time series prediction accuracy using ensemble empirical mode decomposition and recurrent neural networks. *IEEE Access*, *8*, 117133–117145.
Chang, E. C., Cheng, J. W., & Khorana, A. (2000). An examination of herd behavior in equity markets: An international perspective. *Journal of Banking & Finance*, *24*(10), 1651–1679.
Chevalier, J., & Ellison, G. (1999). Career concerns of mutual fund managers. *Quarterly Journal of Economics*, *114*(2), 389–432.
Choe, H., Kho, B.-C., & Stulz, R. M. (1999). Do foreign investors destabilize stock markets? The Korean experience in 1997. *Journal of Financial Economics*, *54*(2), 227–264.
Christie, W. G., & Huang, R. D. (1995). Following the pied piper: Do individual returns herd around the market? *Financial Analysts Journal*, *51*(4), 31–37.
Cipriani, M., & Guarino, A. (2014). Estimating a structural model of herd behavior in financial markets. *American Economic Review*, *104*(1), 224–251.
Clark, P. K. (1973). A subordinated stochastic process model with finite variance for speculative prices. *Econometrica*, *41*, 135–155.
Clements, A., Hurn, S., & Shi, S. (2017). An empirical investigation of herding in the U.S. stock market. *Economic Modelling*, *67*, 184–192.
Cohen, G. (2022). Algorithmic trading and financial forecasting using advanced artificial intelligence methodologies. *Mathematics*, *10*(18), 3302.
Cont, R. (2001). Empirical properties of asset returns: Stylized facts and statistical issues. *Quantitative Finance*, *1*, 223–236.
Cui, Y., Gebka, B., & Kallinterakis, V. (2019). Do closed-end fund investors herd? *Journal of Banking & Finance*, *105*, 194–206.
Dalko, V., Klein, L. R., Sethi, S. P., & Wang, M. H. (2016). Existence of monopoly in the stock market. In A. G. Malliaris, L. Shaw, & H. Shefrin (Eds.), *The global financial crisis and its aftermath hidden factors in the meltdown* (pp. 1–30). Oxford University Press.
Dalko, V., & Wang, M. H. (2019). Volume limit: An effective response to the India flash crash? *Journal of Financial Regulation*, *5*(2), 249–255.
Dalko, V., & Wang, M. H. (2020). High-frequency trading: Order-based innovation or manipulation? *Journal of Banking Regulation*, *21*, 289–298.
Dasgupta, A., Prat, A., & Verardo, M. (2011). Institutional trade persistence and long-term equity returns. *The Journal of Finance*, *66*(2), 635–653.
Devenow, A., & Welch, I. (1996). Rational herding in financial economics. *European Economic Review*, *40*(3–5), 603–615.
Di Giovanni, J., & Hale, G. (2022). Stock market spillovers via the global production network: Transmission of US monetary policy. *The Journal of Finance*, *77*(6), 3373–3421.
Diebold, F. X., & Shin, M. (2017). Assessing point forecast accuracy by stochastic error distance. *Econometric Reviews*, *36*, 588–598.
Dorn, D., Huberman, G., & Sengmueller, P. (2008). Correlated trading and returns. *The Journal of Finance*, *63*(2), 885–920.
Easley, D., Lopez, M. M., & OHara, M. (2012). The volume clock: Insights into the high frequency paradigm. *The Journal of Portfolio Management*, *39*, 19–29.
Filip, A., & Pochea, M. M. (2023). Intentional and spurious herding behavior: A sentiment driven analysis. Journal of behavioral and experimental finance. *Journal of Behavioral and Experimental Finance*, *38*, Article 100810.
Foucault, T., Kozhan, R., & Tham, W. W. (2017). Toxic arbitrage. *The Review of Financial Studies*, *30*(4), 1053–1094.
Galariotis, E. C., Rong, W., & Spyrou, S. I. (2015). Herding on fundamental information: A comparative study. *Journal of Banking & Finance*, *50*, 589–598.
Gavriilidis, K., Kallinterakis, V., & Ferreira, M. P. L. (2013). Institutional industry herding: intentional or spurious? *Journal of International Financial Markets, Institutions and Money*, *26*, 192–214.
GFD (2009). *A comprehensive economic and financial time-series database covering 150 countries and 6,500 different data series*: *Technical report*, Global Financial Data.
Golan, A., & Maasoumi, E. (2008). Information theoretic and entropy methods: An overview. *Econometric Reviews*, *27*(4–6), 317–328.
Gospodinov, N., & Maasoumi, E. (2021). Generalized aggregation of misspecified models: With an application to asset pricing. *Journal of Econometrics*, *222*(1), 451–467.
Gua, Z.-Y. (2017). Heavy-tailed distributions and risk management of equity market tail events. *Journal of Risk and Control*, *4*(1), 31–41.
Hansen, B. E. (1994). Autoregressive conditional density estimation. *International Economic Review*, *35*, 705–730.
Hansen, J., Schmidt, C., & Strobel, M. (2004). Manipulation in political stock markets: Preconditions and evidence. *Applied Economics Letters*, *11*(7), 459–463.
Hashemi, R. R., Ardakani, O. M., Young, J. A., & Bahrami, A. G. (2022). An RNN model for exploring the macroeconomic and financial indicators in the context of the COVID-19 pandemic. In *Proceedings of the international conference on computational science and computational intelligence*, *Proceedings of the international conference on computational science and computational intelligence* (pp. 653–658).
Hirshleifer, D. (2001). Investor psychology and asset pricing. *The Journal of Finance*, *56*(4), 1533–1597.
Hirshleifer, D., Lim, S. S., & Teoh, S. H. (2009). Driven to distraction: Extraneous events and underreaction to earnings news. *The Journal of Finance*, *64*(5), 2289–2325.
Hirshleifer, D., Lourie, B., Ruchti, T. G., & Truong, P. (2021). First impression bias: Evidence from analyst forecasts. *Review of Finance*, *25*(2), 325–364.
Hirshleifer, D., Subrahmanyam, A., & Titman, S. (1994). Security analysis and trading patterns when some investors receive information before others. *The Journal of Finance*, *49*(5), 1665–1698.
Hirshleifer, D., & Teoh, S. H. (2017). How psychological bias shapes accounting and financial regulation. *Behavioural Public Policy*, *1*(1), 87–105.
Housego, L. (2020). Research tests computer-driven crash theory. *Australian Financial Review*.
Hwang, S., & Salmon, M. (2001). A new measure of herding and empirical evidence for the US, UK, and South Korean stock markets. *Financial Econometrics Research Centre*, *1*, 12.
Hyndman, R. J., & Khandakar, Y. (2008). Automatic time series forecasting: The forecast package for r. *Journal of Statistical Software*, *27*(3), 1–22.
Indars, E. R., Savin, A., & Lubloy, A. (2019). Herding behaviour in an emerging market: Evidence from the moscow exchange. *Emerging Markets Review*, *38*, 468–487.

Jiang, G., Mahoney, P. G., & Mei, J. (2005). Market manipulation: A comprehensive study of stock pools. *Journal of Financial Economics*, *77*(1), 147–170.

Khwaja, A. I., & Mian, A. (2005). Unchecked intermediaries: Price manipulation in an emergin stock market. *Journal of Financial Economics*, *78*(1), 203–241.

Kizys, R., Tzouvanas, P., & Donadelli, M. (2021). From COVID-19 herd immunity to investor herding in international stock markets: The role of government and regulatory restrictions. *International Review of Financial Analysis*, *74*, Article 101663.

Klein, L. R., Dalko, V., & Wang, M. H. (2012). Regulating competition in stock markets: Antitrust measures to promote fairness and transparency through investor protection and crisis prevention. Wiley.

Kullback, S. (1959). *Information theory and statistics*. New York: Wiley.

Kullback, S., & Leibler, R. (1951). On information and sufficiency. *The Annals of Mathematical Statistics*, *22*, 79–86.

Kwiatkowski, D., Phillips, P. C. B., Schmidt, P., & Shin, Y. (1992). Testing the null hypothesis of stationarity against the alternative of a unit root. *Journal of Econometrics*, *54*, 159–178.

Maasoumi, E., & Racine, J. S. (2008). A robust entropy-based test of asymmetry for discrete and continuous processes. *Econometric Reviews*, *28*(1–3), 246–261.

Maasoumi, E., & Racine, J. S. (2016). A solution to aggregation and an application to multidimensional 'well-being'frontiers. *Journal of Econometrics*, *191*(2), 374–383.

Maasoumi, E., & Wang, L. (2019). The gender gap between earnings distributions. *Journal of Political Economy*, *127*(5), 2438–2504.

Mandelbrot, B., & Taylor, H. M. (1967). On the distribution of stock price differences. *Operations Research*, *15*, 985–1188.

Mansurov, K., Semenov, A., Grigoriev, D., Radionov, A., & Ibragimov, R. (2023). Impact of self-learning based high-frequency traders on the stock market. *Expert Systems with Applications*, *232*, Article 120567.

Merli, M., & Roger, T. (2013). What drives the herding behavior of individual investors? *Finance*, *34*(3), 67–104.

Racine, J. S., & Maasoumi, E. (2007). A versatile and robust metric entropy test of time-reversibility, and other hypotheses. *Journal of Econometrics*, *138*(2), 547–567.

Roider, A., & Voskort, A. (2016). Reputational herding in financial markets: A laboratory experiment. *Journal of Behavioral Finance*, *17*(3), 244–266.

Rossi, M., Deis, G., Roche, J., & Przywara, K. (2015). Recent civil and criminal enforcement action involving high frequency trading. *Journal of Investment Compliance*, *16*(1), 5–12.

Saha, A., Malkiel, B. G., & Rinaudo, A. (2019). Has the VIX index been manipulated? *Journal of Asset Management*, *20*(1), 1–14.

Shiller, R. J. (2000). *Irrational exuberance*. Princeton: Princeton University Press.

Sias, R. W. (2004). Institutional herding. *The Review of Financial Studies*, *17*(1), 165–206.

Smith, L., Sorensen, P. N., & Tian, J. (2021). Informational herding, optimal experimentation, and contrarianism. *Review of Economic Studies*, *88*(5), 2527–2554.

Soofi, E. S. (1994). Capturing the intangible concept of information. *Journal of the American Statistical Association*, *89*, 1243–1254.

Soofi, E. S., & Retzer, J. J. (2002). Information indices: unification and applications. *Journal of Econometrics*, *107*, 17–40.

Tan, L., Chiang, T. C., Mason, J. R., & Nelling, E. (2008). Herding behavior in Chinese stock markets: An examination of a and b shares. *Pacific-Basin Finance Journal*, *16*(1–2), 61–77.

Tan, L. P., Sadiq, M., Aldeehani, T. M., Ehsanullah, S., Mutira, P., & Vu, H. M. (2021). How COVID-19 induced panic on stock price and green finance markets: global economic recovery nexus from volatility dynamics. *Environmental Science and Pollution Research*, 1–14.

Vayanos, D., & Woolley, P. (2013). An institutional theory of momentum and reversal. *The Review of Financial Studies*, *26*(5), 1087–1145.

Venezia, I., Nashikkar, A., & Shapira, Z. (2011). Journal of banking & finance. *Journal of Banking & Finance*, *35*, 1599–1609.

Welch, I. (1992). Sequential sales, learning, and cascades. *The Journal of Finance*, *47*(2), 695–732.

Wermers, R. (1999). Mutual fund herding and the impact on stock prices. *The Journal of Finance*, *54*(2), 581–622.